

## Response to Reviewer

19 December 2024

### Overview:

The authors evaluated five diagnosis schemes of identifying winter precipitation types using data from the ICE-POP 2018 field experiment. They found that the scheme using one-dimensional spectral bin model (SBM) with the climatological snow density-diameter relationship for the Pyeongchang region demonstrates superior performance. The manuscript is well written, clear, and easy to follow. I have only some minor comments regarding clarification or justification for consideration.

Dear Referee,

We greatly appreciate your positive feedback and the time and effort you devoted to reviewing our manuscript and dataset. We have carefully reviewed your comments and actively reflected them. Thank you again for your help in improving our manuscript.

Best regards,

Wonbae Bang (on behalf of the author team)

## Specific Comments:

1. Section 2.2: How large uncertainties of these observations? The authors should discuss them to enhance the manuscript's robustness.

→ Thank your advice and I reflect it. I add explanation about measurement errors of PARSIVEL and sounding. Also, specification of MRR is more detailed at Section 2.2.

(red color letter between 130~150 lines of revision file)

### 2.2 Observational data and quality control

A PARSIVEL is a disdrometer that uses a laser beam with a wavelength of 780 nm to obtain a particle's equivolume diameter ( $D$ , mm) and fall velocity ( $V_f$ ,  $\text{m s}^{-1}$ ) based on changes in the laser beam signals. The measurable range of  $D$  ( $V_f$ ) is from 0.3 mm ( $0.1 \text{ m s}^{-1}$ ) to 30 mm ( $20 \text{ m s}^{-1}$ ). The overall error of  $D$  is within 5% and  $V_f$  has errors ranging from 10 % to 25% as  $D$  changes (Löffler-Mang and Joss, 2000). We suggest how to deal with these measurement errors in Section 3.1. Version 2 PARSIVELs and level 1 data are used in the present study. Level 1 data are format-converted with no processing and provide particle counts for individual diameter and velocity channels (a 32 by 32 array) every 1 min. Because the observed PARSIVEL data contain outliers that may be the result of various forms of error, such as calibration errors and "margin fallers" (Yuter et al., 2006), we eliminate any of the level 1 data that meet one or both of the following two criteria: i)  $D < 1 \text{ mm}$  and ii)  $V_f > 1.4V_a$ .  $V_a$  is the empirical relationship between  $D$  and  $V_f$  established by Atlas et al. (1973).

A modern-type rawinsonde (M10) is used for the ICE-POP 2018 campaign (In et al., 2018). The observation variables recorded by the M10 rawinsonde are pressure ( $P$ , hPa),  $T$  ( $^{\circ}\text{C}$ ), RH (%), wind speed (WS,  $\text{m s}^{-1}$ ) and wind direction (WD,  $^{\circ}$ ) at 1 s intervals. Additionally,  $T_w$  is calculated using the two-parameter relationship for  $T$  and RH suggested by Stull (2011). Although rawinsonde data is useful as a reference of atmospheric vertical structure, the absolute accuracy of  $T$  and RH of the M10 rawinsonde sensor are  $0.3^{\circ}\text{C}$  and 3%, respectively (In et al. 2018). The impact of these measurement errors can be significant near  $0^{\circ}\text{C}$ , where phase changes of precipitation particles occur.

The MRRs are modulated continuous wave (FMCW) radar instruments using a solid-state transmitter with a frequency of 24 GHz (Maahn and Kollias, 2012). In this study, the range resolution of the MRRs is set to 150 m. This resolution is enough to identify the ML because the average ML depth based on dual-polarization radar measurements from the Korean peninsula during winter is about 670 m (Allabakash et al. 2019). Raw data from MRR supplies vertical profiles of radar reflectivity ( $Z$ , dBZ) and Doppler velocity ( $V_r$ ,  $\text{m s}^{-1}$ ) in precipitation.  $Z$  and  $V_r$  can be contaminated by noise including non-meteorological echoes. Also, if  $V_r$  exceeds the Nyquist velocity boundaries ( $-6 \text{ m s}^{-1} \sim 6 \text{ m s}^{-1}$ ) of the MRR, aliasing of  $V_r$  will occur (Maahn and Kollias, 2012). In general, large raindrops in heavy rainfall events cause the aliased data. Therefore, raw data from the MRRs are quality-controlled using de-aliasing and the noise removal algorithm suggested by Maahn and Kollias (2012). The processed MRR data are used to provide additional context for important cases in the present study.

**2. Lines 156-162: Was there only one sounding available for each precipitation event? Should the earlier soundings be used as environmental profiles to diagnose precipitation types?**

→ Yes. One event is only one sounding data. If precipitation is identified by PARSIVEL when sounding launches at specific time and site, the event includes matched precipitation case (The explanation about selection of 'matched precipitation case' is added at main contents). 'Winter precipitation type' is mainly decided by low-level atmospheric condition (melting layer, freezing layer, inversion layer, saturation layer, and so on). Low-level atmospheric condition is very changeable. Therefore, when precipitation occurs, it is appropriate to use sounding data from the nearest time or the current time for diagnosis. Sounding data of current time in this study was used.

(red color letter between 174~175 lines of revision file)

We obtain a total of 131 matched precipitation cases to validate the five diagnostic methods during the ICE-POP period (1 November 2017–30 April 2018). **If precipitation is identified when a sounding launches at a specific time and site, the event includes a matched precipitation case.** Cases are identified that feature measurable precipitation at each of the five sounding sites. We identify precipitation cases at each site that satisfy two conditions: i)  $N_{RA} + N_{SN} \geq 15$  within 5 min of the sounding start time, and ii)  $-4\text{ °C} < T_0 < 6\text{ °C}$  and  $RH_0 > 40\%$  at the sounding start time. Here,  $T_0$  and  $RH_0$  are the data recorded 1 s after the start of the sounding, and they accurately represent the surface  $T$  and RH measured by the rawinsonde. Based on this hydrometeor-type classification scheme, the dominant WPT of the matched precipitation cases is determined using the newly developed algorithm with the quality-controlled 5 min PARSIVEL data (Fig. 2b).

**3. Lines 221-222: How to determine critical values for different sites? Please clarify.**

→ Thank your advice and I reflect it. The same critical value was used for sites with similar terrain characteristics. I add supplementary explanation at main contents.

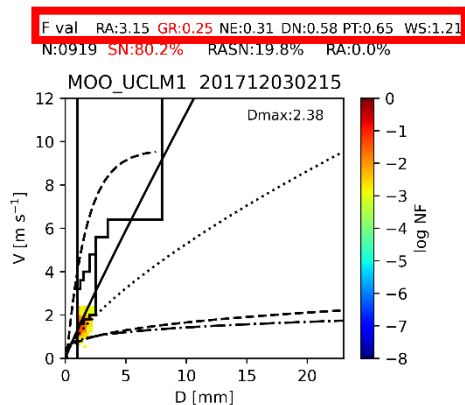
(red color letter between 241~243 lines of revision file)

gpm, respectively. The WPTs at GWU, BKC, and SCW are diagnosed using the former critical values, while DGW and MOO are diagnosed using the latter. **The reason for using different critical values is that GWU, BKC, and SCW are located near the East sea at a low altitude and east of the Taebaek mountains whereas DGW and MOO are located within the Taebaek mountains and have a relatively higher altitude (Fig. 1a).**

4. Lines 293-294: Please justify “initialized as unrimed low-density snow aggregates”.

→ Thank advice, I should add explanation. In this study, Number of SN events is 91, graupel-like events is only 13 events and not-graupel events is 78. We can divide this by using ‘F val’. You can see results at “Surface precipitation type based on new decision algorithm about 131 precipitation events in 5 ICE-POP 2018 sites” asset <https://doi.org/10.5281/zenodo.13561536>

In the fig (PARSIVEL V-D scatterplot of each event), you can see ‘F val’.



We calculated ‘F val’ following Lee et al. (2015), ‘F val’ quantifies difference between data and empirical relationship. So, F value is smallest, it is dominant hydrometeor (marks red color).

I added explanation at main contents.

(red color letter between 315~317 lines of revision file)

315 The SBM parameters used in this study are presented in Table 2. The particles are separated into 20 size bins and initialized as ‘unrimed low-density snow aggregates’ because there are only 13 graupel-like events among the 91 SN events following the hydrometeor classification method suggested by Lee et al. (2015). The size bins are delineated such that the equivolume diameters of fully melted particles of equal mass in each bin are 0.1 mm apart. The largest size bin used in this study, with a fully melted equivolume diameter  $D_{mw,max}$  of 1.95 mm, is about 2 times the mean value of the mass-weighted mean diameter

Lee, J. E., Jung, S. H., Park, H. M., Kwon, S., Lin, P. L., and Lee, G.: Classification of precipitation types using fall velocity-diameter relationships from 2D-video distrometer measurements, Adv. Atmos. Sci., 32, 1277-1290., <https://doi.org/10.1007/s00376-015-4234-4>, 2015.

**5. Lines 298-303: The authors argued that “the assumption of mass conservation” may be valid. However, how about PSDs? Given the same mass, PSDs at the surface and in the upper atmosphere could differ significantly. Please justify it.**

→ Yes, actually, PSD during falling is very changeable and continuously evolved by many microphysical processes (aggregation, riming, and so on). And, aircraft microphysics data is very useful for initial PSD. However, aircraft microphysics data is very lack during ICE-POP period. Also, current SBM scheme not include aggregation and riming process. I add sentence about this situation at main content.

(red color letter between 327~328 lines of revision file)

325 evaporation/sublimation) for simplicity and instead only consider melting/refreezing. The assumption of mass conservation should generally be valid for this study because almost all of the precipitation cases are nearly saturated ( $RH > 80\%$ ) below 5 km AGL (Fig. 5b). **The initial PSD is fixed for all events because of the lack of aircraft microphysical observation data and the exclusion of aggregation/riming process in the microphysics scheme in the current SBM.**

**6. Figures 10-12: Which SBM method, original or optimized one is shown in these figures?**

→ Thank your check. I specifies it at caption in Fig. 10.

And, from request of editor (specify model 'version'), model version is specified in introduction section. SBM have 3 versions:

- 1) Reeves et al (2016): origin version
- 2) Carlin et al (2019): 1DSBM-19 (upgrade of Reeves et al. 2016)
- 3) This study: 1DSBM-19M (modified version of Carlin et al. 2019)

Because 'original SBM' in from 'data' section to 'summary and future work' section means 1DSBM-19M, I change expression 'original SBM' to 'current SBM'.

(red color letter between 478 line of revision file)

475

$T_w$  [°C]

**Figure 10.  $T_w$  profiles for observed SN cases occurring at (a) mountain sites and (b) coastal sites. The blue, red, and green lines indicate diagnosed RA, SN, and RASN cases, respectively, for the  $H_{850}$  thickness, shifted Matsuo scheme on  $RH_0 - T_0$  nomogram, wet-bulb temperature  $T_{w0}$ ,  $T_{w0} - \Gamma_{low}$  nomogram, and the **current** SBM methods. Bold lines indicate misdiagnosed cases.**

**7. Line 500: Why were not all examples within each group included, especially given the limited number of examples? A justification for this selection would be helpful.**

→ A representative example from each group is only shown because each group have similar atmospheric environmental characteristics (I add this sentence at main contents). Testing was conducted at all eight misdiagnosed cases. Simulation results (correct/not correct of precipitation type) of eight misdiagnosed cases was mentioned at 584~585 lines (revision file):

'Among the eight misdiagnosed cases in the SBM, four are correctly diagnosed by the optimized SBM. If a more accurate 585 cloud top is also considered, two more cases are correctly diagnosed by the optimized SBM.)'

(red color letter between 525~526 lines of revision file)

525 Only a representative example from each group is shown because each group has similar atmospheric environmental characteristics. We also compare the simulation results between the current and optimized SBMs. Figure 13 presents the environmental profiles from the rawinsondes and  $V_T-D$  scatterplots from the corresponding PARSIVEL taken at around 1200

**8. Lines 546-547: Should the authors also consider updating the  $V_T-D$  relationship for ice particles?**

→ Although event 3 at Fig.14 was not refreezing event (based on Fig. 15), I also think evaluation of SBM microphysics scheme about ice pellet event will be required. I add this at 'summary and future work' section.

(red color letter between 618~619 lines of revision file)

The potential of the SBM for diagnosing the WPT was thus confirmed in the present study. The performance of the current SBM was superior to existing optimized methods (the  $H_{850}$  and  $RH_0-T_0$  nomogram methods) and the skill scores were improved further via regional optimization of the SBM's microphysics scheme. Furthermore, there is a need to verify the microphysics

---

scheme in the SBM in more detail, such as for IP events and so on. We will focus on the development of a combined SBM  
620 with other reanalysis field data for the acquisition of three-dimensional WPT information.